Supporting Online Material for

Wind-Driven Upwelling in the Southern Ocean and the Deglacial Rise in Atmospheric CO$_2$

R. F. Anderson,[*] S. Ali, L. Bradtmiller, S. H. H. Nielsen, M. Q. Fleisher, B. E. Anderson, L. H. Burckle

*To whom correspondence should be addressed. E-mail: boba@ldeo.columbia.edu

This PDF file includes:

SOM Text
Figs. S1 to S4
Tables S1 to S4
References

Supporting Online Material

Age model for E27-23

        A rough age model for the core was first established by counting the relative abundance of *Eucampia antarctica*, expressed as percentage of total diatoms. Within a given core from the Southern Ocean, the percent abundance of *E. antarctica* is typically severalfold greater during glacial periods than during interglacials (*S1, S2*). In the absence of overriding evidence to the contrary, the uppermost peak in the downcore record of *E. antarctica* abundance is typically assigned an age corresponding to the most extreme conditions of the Last Glacial Period (roughly 18,000 to 28,000 years BP).

        Sediment samples from E27-23 were processed as described in Burckle et al. (*S3*). Duplicate microscope slides were prepared from each sample and a minimum of 300 diatom valves were counted in each slide to determine the relative abundance of *E. antarctica.* Results are presented in Table S1 and in Figure S1. The abundance peak at approximately 800 cm is inferred to represent the peak of the Last Glacial Period.

        After identifying the Last Glacial Period, the age model was refined by obtaining radiocarbon ages on mixed planktonic foraminifera tests (Table S2). Samples for radiocarbon were disaggregated using distilled water, and sieved. The >250μm size fraction was picked first, and supplemented by tests from the >150μm size fraction when necessary. Radiocarbon measurements were performed at the National Ocean Sciences Accelerator Mass Spectrometry Facility (NOSAMS). Radiocarbon ages were converted to calendar ages using the CALIB 5.0 program (*S4*) and the Marine calibration curve (*S5*). Reservoir corrections for Southern Ocean surface waters during the last glacial period have not been constrained, although they are believed to be substantially greater than the standard reservoir correction of 400 years. Consequently, an additional correction of 800 ± 200 years was applied in calculating calendar ages.

Correlation with deep North Atlantic conditions

        Rickaby and Elderfield (*S6*) interpreted the carbon isotopic composition of benthic foraminifera (*C. wuellerstorfi*) in the high-latitude North Atlantic core NEAP4k (61° 29'N, 24° 10'W, 1627 m) to indicate the presence of southern source deep water at this location during time intervals surrounding Heinrich Event 1 (HE1) and the Younger Dryas (YD). The pattern of variability in the carbon isotope record from NEAP4k is similar to that of the opal flux proxy for upwelling in the Southern Ocean (Figure S2). For example, the sharp rise in opal flux early in the deglacial corresponds to a reduction (note the reversed scale) in $\delta^{13}C$ at the site of NEAP 4k. Reduced opal flux during the Antarctic Cold Reversal (ACR; see main text) corresponds to a temporary rise in $\delta^{13}C$, while renewed upwelling (opal flux) in the Southern Ocean following the ACR corresponds to another drop in $\delta^{13}C$ in the NEAP 4k record. The slight offset in the records could reflect the uncertainty in the age model of either core.

        The intrusion of southern source waters during intervals surrounding HE1 and the YD can be linked to the contemporary reduction in the formation of North Atlantic Deep water (*S7*), which allowed the chemical signature of nutrient-rich ^{13}C-depleted Southern Ocean water to mix throughout the deep North Atlantic basin.

Age model for TN057-14PC

An age model for this core was based on a high-resolution record of the relative abundance of *Eucampia antarctica*, expressed as percentage of total diatoms. Sediment samples from TN057-14PC were processed as described above for E27-23. Results are presented in Table S3.

As noted above, the percent abundance of *E. antarctica* is typically greater during glacial periods than during interglacials (*S1, S2*). Assuming that the relative abundance of *E. antarctica* is correlated with temperature over Antarctica, we constructed an age model for TN057-14PC on the GISP-II time scale by correlating features in the *E. antarctica* record with corresponding features in the record of oxygen isotope composition of benthic foraminifera in core MD95-2042 from the Iberian margin (*S8*). An age model for MD95-2042 on the GISP-II time scale has been developed by correlating features in the oxygen isotopic record of planktonic foraminifera with the oxygen isotope record of the GISP-II ice core, which is interpreted to reflect temperature over Greenland. The age model for MD95-2042 was originally based on the GRIP time scale (*S8*), and later adjusted to the GISP-II time scale. The GISP-II age model and isotope data for MD95-2042 are available at: ftp://ftp.ncdc.noaa.gov/pub/data/paleo/contributions_by_author/shackleton2000/.

The oxygen isotope record of benthic foraminifera in MD95-2042 clearly delineates the seven warm events in Antarctica during the last glacial period as first identified in ice core records (*S9*). These warm events (A1 - A7) are marked on the oxygen isotope record of MD95-2042 in Fig. S3A. Similar features are observed in the *E. antarctica* record of TN057-14PC (Fig. S3B). Tie lines in Fig S3 indicate our choices for age control points (Table S4) used to develop an age model for TN057-14PC on the GISP-II time scale.

Nielsen et al. (*S10*) presented an age model for TN057-14PC based on radiocarbon ages and oxygen isotopes measured on planktonic foraminifera (*Neogloboquadrina pachyderma*). The age model derived by correlating *E. antarctica* abundance with the oxygen isotope record of MD95-2042 agrees well (Fig. S4) with the age model of Nielsen et al. (*S10*). Subtle differences exist between 40 and 50 ka (i.e., approximately 700 to 1000 cm), where there appears to be a greater accumulation rate in the age model based on ^{14}C and ^{18}O, as well as at the base of the core. We chose to use the age model based on *E. antarctica* because radiocarbon dating is pushed to its extreme limits in the 40 to 50 ka time interval. Good agreement between these two age models, which are based on entirely different approaches, lends confidence to the accuracy of the ages and further supports the principle that the relative abundance of *E. antarctica* can be used to construct reliable age models in Southern Ocean sediments (*S1, S2*).
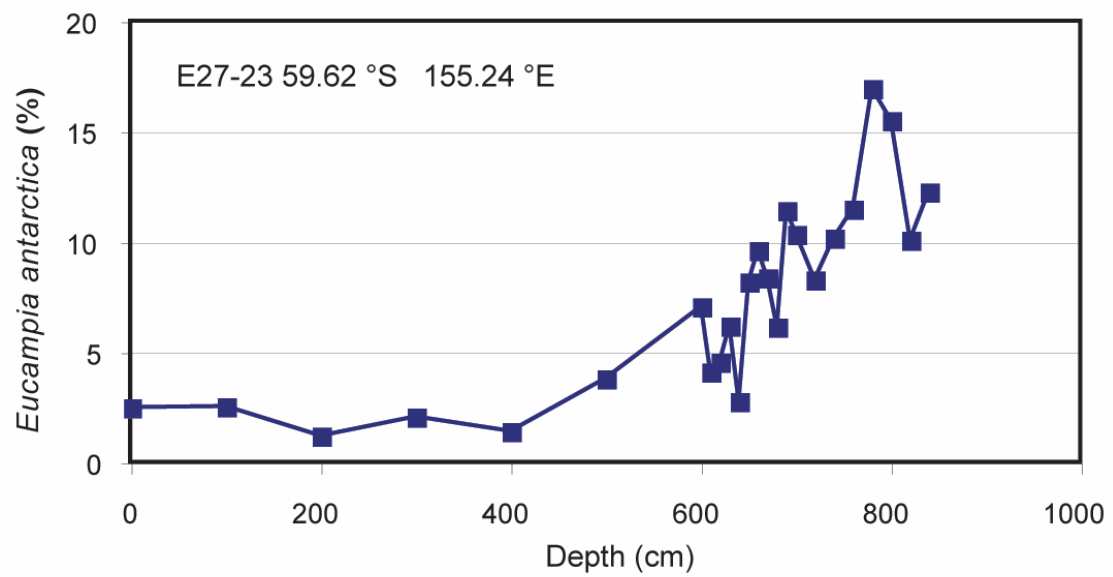
Figure S1. Relative abundance of *Eucampia antarctica*, expressed as percentage of total diatoms, in samples from core E27-23. The peak abundance at ~800 cm is inferred to represent the most extreme conditions of the Last Glacial Period, roughly 18 ka - 28 ka. Results are presented in Table S1.
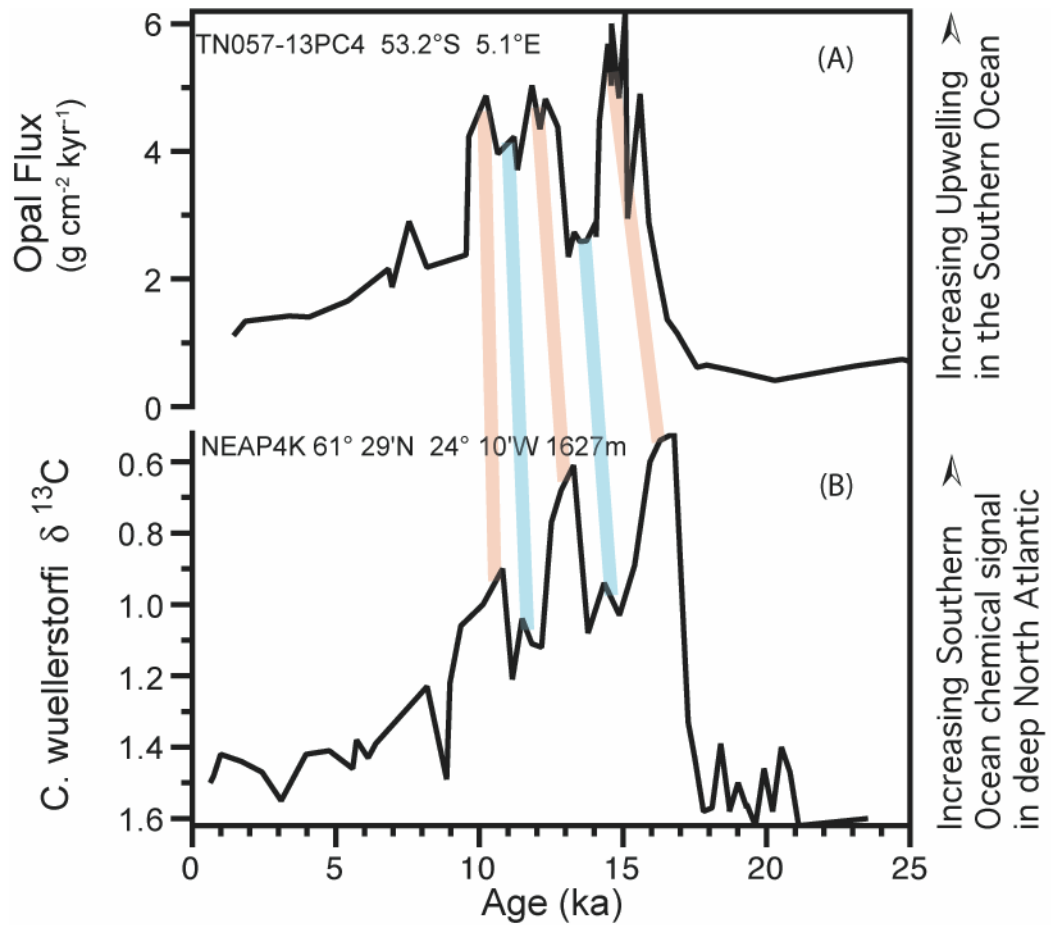
Figure S2. (A) Opal flux in core TN057-13 4PC, interpreted to represent a proxy for upwelling in the Southern Ocean (see main text). (B) Carbon isotopic composition of benthic foraminifera (*C. wuellerstorfi*) in high-latitude North Atlantic core NEAP 4k (*S6*). The similar pattern of variability in the two records supports the view that nutrient-rich ^{13}C-depeted water characteristic of the Southern Ocean mixed throughout the deep North Atlantic Basin during intervals surrounding Heinrich Event 1 and the Younger Dryas, when formation of North Atlantic Deep water is thought to have been greatly reduced (*S7*). Tie lines indicate features that are inferred to be correlated. Temporal offsets may reflect uncertainties in the age model of either core.
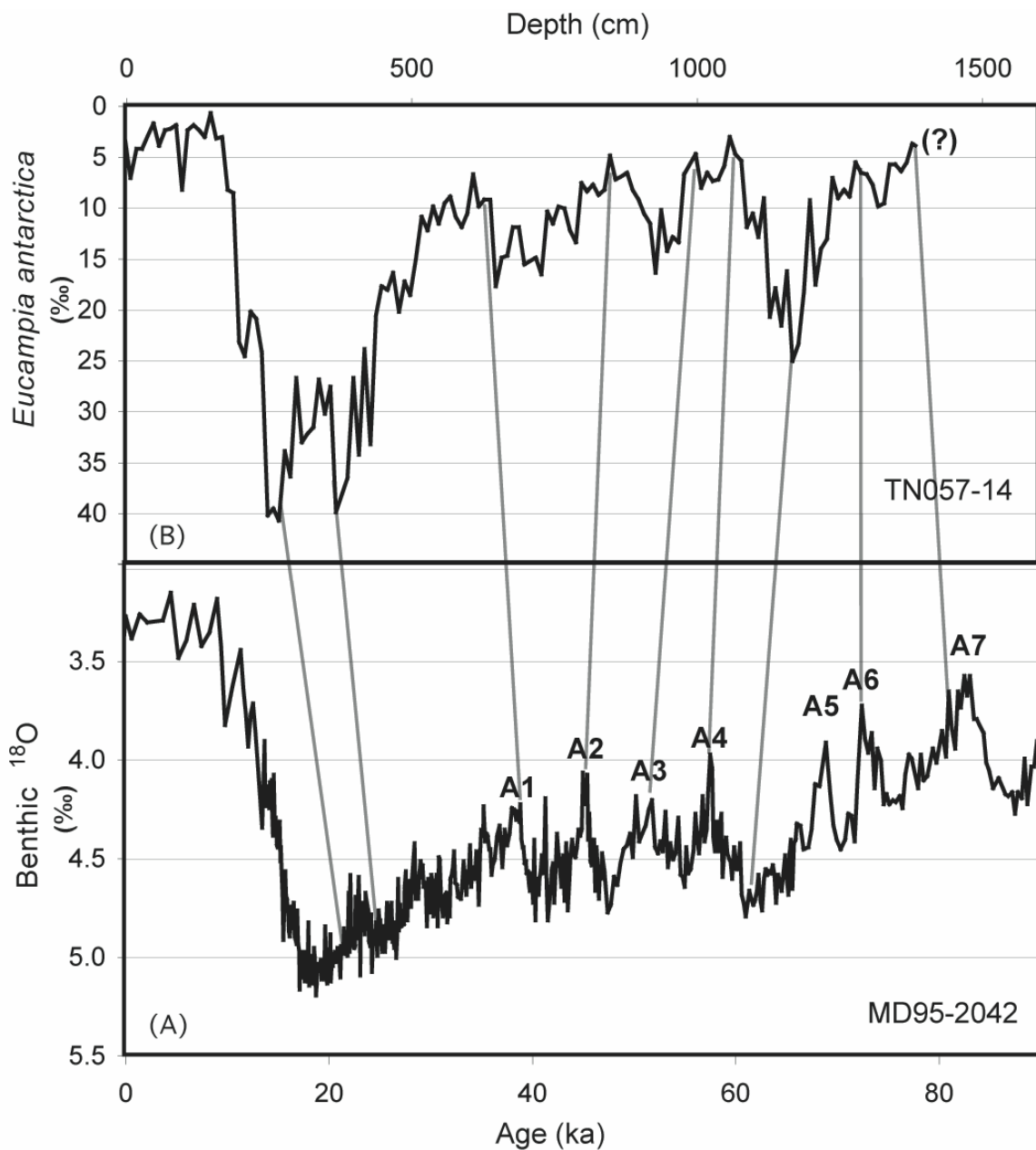
Figure S3. (A) Oxygen isotope record from benthic foraminifera in core MD95-2042 on the GISP-II time scale (see text). Minima (note reversed scale) correlated to Antarctic warm events A1 - A7 (*S9*) are marked. (B) Relative abundance of *Eucampia antarctica* in core TN057-14-4PC (51° 59.059'S 4° 30.976'E 3648 m) plotted against depth in core. Minimum relative abundances (note reversed scale) are correlated with warm intervals. Grey lines indicate age control points used to develop an age model for TN057-14 on the GISP-II time scale (Table S4).
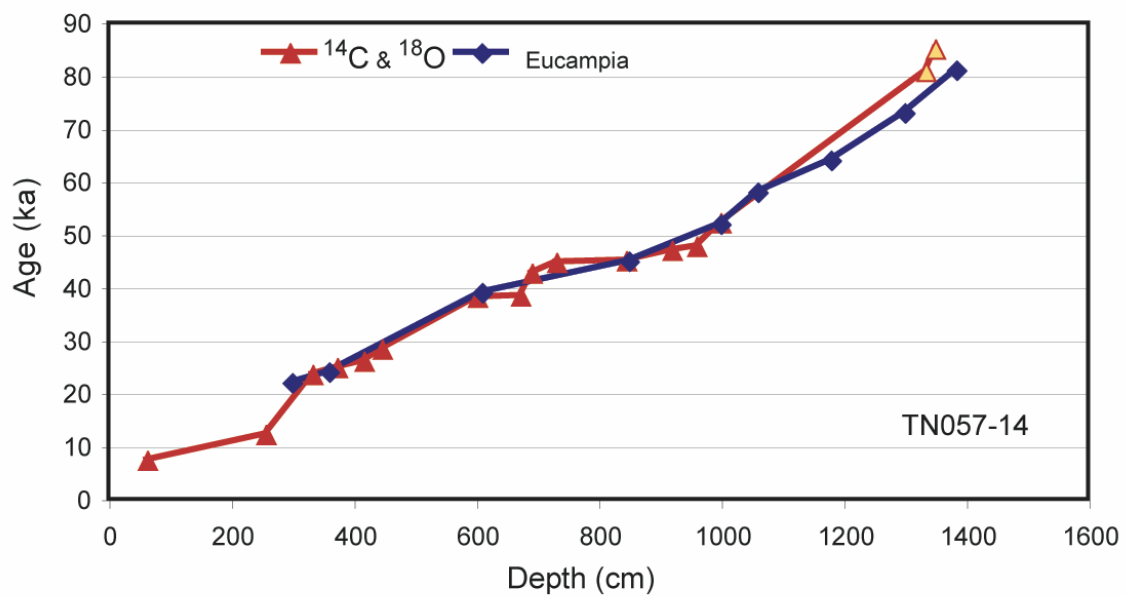
Figure S4. Age-depth relationship for TN057-14 based on age control points in Table S4 (blue diamonds) compared to the published relationship (red triangles based on ^{14}C; red triangle with yellow fill based on ^{18}O) (*S10*).

Table S1.   Relative abundance of *Eucampia antarctica* in samples from core E27-23.
             Results represent counts of at least 300 valves from duplicate microscope slides.

| Depth (cm) | Slide 1 | | | | Slide 2 | | | Average |
	E. antarctica	Total	percent E.A.	*E. antarctica*	Total	percent E.A.	*E. antarctica (%)*
0-1	8	334	2.4	8	308	2.6	2.5
100-101	7	303	2.3	9	326	2.8	2.5
200-201	7	338	2.1	1	314	0.3	1.2
300-301	6	302	2.0	7	328	2.1	2.1
400-401	3	307	1.0	6	325	1.8	1.4
500-501	12	326	3.7	13	333	3.9	3.8
600-601	22	304	7.2	21	305	6.9	7.1
610-611	11	319	3.4	15	316	4.7	4.1
620-621	15	305	4.9	13	312	4.2	4.5
630-631	20	308	6.5	18	306	5.9	6.2
640-641	11	307	3.6	12	609	2.0	2.8
650-651	26	321	8.1	25	302	8.3	8.2
660-661	30	320	9.4	30	304	9.9	9.6
670-671	26	314	8.3	30	355	8.5	8.4
680-681	19	307	6.2	19	311	6.1	6.1
690-691	35	335	10.4	43	347	12.4	11.4
700-701	35	309	11.3	29	310	9.4	10.3
720-721	27	307	8.8	25	322	7.8	8.3
740-741	38	334	11.4	28	312	9.0	10.2
760-761	42	304	13.8	29	316	9.2	11.5
780-781	59	309	19.1	45	304	14.8	16.9
800-801	42	316	13.3	53	299	17.7	15.5
820-821	29	317	9.1	34	309	11.0	10.1
840-841	37	305	12.1	38	307	12.4	12.3

Table S2. Radiocarbon ages for mixed planktonic foraminifera and conversion to calendar age.
All cores are E27-23. An excess reservoir correction of 800±200 years was applied.

Lab code	Description	^{14}C Age (years BP)	^{14}C Age SD (years)	CALIB 5.0.1[1] (cal yr-)	CALIB 5.0.1 (cal yr+)	CALIB 5.0.1 (cal yr avg)
OS- 51913	E27-23 600	12150	60	12773	13120	12915
OS- 51910	E27-23 740	14300	65	15174	15799	15504
OS- 51914	E27-23 760	14850	65	15901	16563	16229
OS- 51915	E27-23 780	18250	95	19939	20389	20183

[1] CALIB = Calendar ages derived using the CALIB radiocarbon calibration program (S4)
   available at http://radiocarbon.pa.qub.ac.uk/calib using the calibration data set
   of Hughen et al. (S5).

Table S3.   Relative abundance of *Eucampia antarctica* from core TN057-14.

Results represent counts of at least 300 valves, normally from duplicate microscope slides.

| | Slide 1 | | | Slide 2 | | | **Average** |
| | | | | | | | *E. antarctica* |
Depth (cm)	# *E antarctica*	Total diatoms	Percent E.A.	# *E antarctica*	Total diatoms	Percent E.A.	*%*
0	10	300	3.33				3.33
10	17	301	5.65	26	300	8.67	7.16
20	13	300	4.33	13	301	4.32	4.33
30	13	300	4.33	13	300	4.33	4.33
40	9	300	3.00				3.00
50	9	301	2.99	2	302	0.66	1.83
60	12	303	3.96				3.96
70	5	300	1.67	10	300	3.33	2.50
80	7	302	2.32				2.32
90	7	301	2.33	5	300	1.67	2.00
100	22	300	7.33	28	300	9.33	8.33
110	8	300	2.67	7	300	2.33	2.50
120	6	300	2.00				2.00
130	9	301	2.99	6	301	1.99	2.49
140	12	300	4.00	7	300	2.33	3.17
150	2	300	0.67	3	300	1.00	0.83
160	10	301	3.32				3.32
170	8	300	2.67	11	301	3.65	3.16
180	21	300	7.00	29	300	9.67	8.33
190	30	301	9.97	22	301	7.31	8.64
200	70	301	23.26				23.26
210	72	300	24.00	76	300	25.33	24.67
220	59	300	19.67	63	301	20.93	20.30
230	61	300	20.33	65	300	21.67	21.00
240	73	300	24.33				24.33
250	123	300	41.00	119	300	39.67	40.33
260	109	300	36.33	129	302	42.72	39.52
270	119	301	39.53	126	300	42.00	40.77
280	102	300	34.00				34.00
290	111	300	37.00	108	300	36.00	36.50
300	81	300	27.00	80	300	26.67	26.83
310	94	302	31.13	105	301	34.88	33.00
320	97	300	32.33				32.33
330	91	300	30.33	99	300	33.00	31.67
340	82	300	27.33	80	301	26.58	26.96
350	94	301	31.23	88	300	29.33	30.28
360	83	301	27.57				27.57
370	124	300	41.33	116	300	38.67	40.00
390	101	300	33.67	119	300	39.67	36.67
400	79	300	26.33	82	300	27.33	26.83
410	104	302	34.44	102	300	34.00	34.22
420	70	301	23.26	74	300	24.67	23.96
430	99	301	32.89	101	300	33.67	33.28
440	62	302	20.53				20.53
450	69	300	23.00	54	300	18.00	20.50
460	53	300	17.67	56	300	18.67	18.17
470	47	301	15.61	52	300	17.33	16.47
480	61	301	20.27				20.27
490	56	300	18.67	48	300	16.00	17.33

500	52	300	17.33	60	300	20.00	18.67
510	44	300	14.67	46	301	15.28	14.97
520	33	300	11.00				11.00
530	41	300	13.67	33	300	11.00	12.33
540	37	302	12.25	23	301	7.64	9.95
550	30	301	9.97	40	301	13.29	11.63
560	29	300	9.67				9.67
570	23	300	7.67	31	300	10.33	9.00
580	35	300	11.67	31	301	10.30	10.98
590	38	300	12.67	34	302	11.26	11.96
600	32	300	10.67				10.67
610	21	300	7.00	20	301	6.64	6.82
620	27	300	9.00	33	302	10.93	9.96
630	26	300	8.67	30	300	10.00	9.33
640	28	302	9.27				9.27
650	65	300	21.67	42	300	14.00	17.83
660	42	300	14.00	48	300	16.00	15.00
670	46	300	15.33	43	301	14.29	14.81
680	34	301	11.30				11.30
690	35	300	11.67	37	300	12.33	12.00
700	50	301	16.61	44	300	14.67	15.64
710	51	300	17.00	41	301	13.62	15.31
720	45	300	15.00				15.00
730	45	301	14.95	55	300	18.33	16.64
740	30	303	9.90	33	300	11.00	10.45
750	33	300	11.00	37	301	12.29	11.65
760	30	303	9.90				9.90
770	33	302	10.93	28	300	9.33	10.13
780	36	301	11.96	38	300	12.67	12.31
790	43	300	14.33	38	300	12.67	13.50
800	23	300	7.67				7.67
810	25	300	8.33	26	301	8.64	8.49
820	23	300	7.67	24	300	8.00	7.83
830	29	300	9.67	24	300	8.00	8.83
840	25	301	8.31				8.31
850	14	300	4.67	16	300	5.33	5.00
860	24	300	8.00	20	301	6.64	7.32
870	22	301	7.31	20	300	6.67	6.99
880	20	300	6.67				6.67
890	26	300	8.67	24	300	8.00	8.33
900	28	300	9.33	28	300	9.33	9.33
910	32	300	10.67	32	300	10.67	10.67
920	35	302	11.59				11.59
930	48	302	15.89	51	300	17.00	16.45
940	32	300	10.67	30	300	10.00	10.33
950	45	300	15.00	41	300	13.67	14.33
960	39	300	13.00				13.00
970	43	301	14.29	38	300	12.67	13.48
980	19	300	6.33	22	300	7.33	6.83
990	18	300	6.00	17	300	5.67	5.83
1000	15	301	4.98	14	300	4.67	4.83
1010	25	300	8.33	24	300	8.00	8.17
1020	17	303	5.61	23	300	7.67	6.64
1030	24	300	8.00	21	300	7.00	7.50
1040	20	300	6.67	24	302	7.95	7.31
1050	20	301	6.64	16	300	5.33	5.99

1060	8	301	2.66	11	300	3.67	3.16
1070	12	300	4.00	17	300	5.67	4.83
1080	20	301	6.64	14	300	4.67	5.66
1090	34	300	11.33	38	300	12.67	12.00
1100	32	300	10.67				10.67
1110	32	300	10.67	46	300	15.33	13.00
1120	27	301	8.97	28	302	9.27	9.12
1130	53	300	17.67	72	300	24.00	20.83
1140	46	301	15.28	62	302	20.53	17.91
1150	61	300	20.33	69	301	22.92	21.63
1160	47	300	15.67	51	303	16.83	16.25
1170	73	301	24.25	78	300	26.00	25.13
1180	67	303	22.11	74	300	24.67	23.39
1190	59	300	19.67	51	300	17.00	18.33
1200	33	302	10.93	23	303	7.59	9.26
1210	55	300	18.33	51	300	17.00	17.67
1220	42	300	14.00	43	301	14.29	14.14
1230	37	300	12.33	42	300	14.00	13.17
1240	19	301	6.31	24	300	8.00	7.16
1250	23	300	7.67	32	300	10.67	9.17
1260	28	300	9.33	22	300	7.33	8.33
1270	25	300	8.33	29	300	9.67	9.00
1280	15	301	4.98	19	301	6.31	5.65
1290	25	300	8.33	21	300	7.00	7.67
1300	18	300	6.00	23	300	7.67	6.83
1310	21	300	7.00	26	300	8.67	7.83
1320	27	302	8.94	33	301	10.96	9.95
1330	25	300	8.33	29	300	9.67	9.00
1340	13	300	4.33	22	300	7.33	5.83
1350	20	300	6.67	15	300	5.00	5.83
1360	18	300	6.00	21	300	7.00	6.50
1370	18	300	6.00	16	300	5.33	5.67
1380	11	301	3.65	12	302	3.97	3.81
1385	14	300	4.67	10	301	3.32	3.99

Table S4.   Age control points for correlating the *Eucampia antarctica* record of TN057-14 with the oxygen isotope record from benthic foraminifera in MD95-2042 on the GISP II time scale (Fig. S3). The age model for MD95-2042 was originally published on the GRIP time scale and later placed on the GISP II time scale, as provided at: ftp://ftp.ncdc.noaa.gov/pub/data/paleo/contributions_by_author/shackleton2000/

Event	MD95-2042 GISP-II age (ka)	TN057-14 Depth (cm)
End Mid LGM warmth	22	300
Start Mid LGM warmth	24	360
Initial A1 ^{18}O minimum	39	610
A2 ^{18}O minimum	45	850
A3 ^{18}O minimum	52	1000
A4 ^{18}O minimum	58	1060
MIS 4 maximum ^{18}O	64	1180
A5 ^{18}O minimum	69	
A6 ^{18}O minimum	73	1300
Late A7 ^{18}O minimum	81	1385

SOM References

S1. L. H. Burckle, R. W. Burak, in *Landscapes and Life. Studies in Honour of Urve Miller* A. M. Robertsson, Ed. (Conseil de l'Europe, Rixensart, Belgium, 1996), vol. PACT 50, pp. 15-22.
S2. L. H. Burckle, D. W. Cooke, *Micropaleontology* **29**, 6 (1983).
S3. L. H. Burckle, D. B. Clarke, N. J. Shackleton, *Geology* **6**, 243 (1978).
S4. M. Stuiver, P. J. Reimer, *Radiocarbon* **35**, 215 (1993).
S5. K. A. Hughen *et al.*, *Radiocarbon* **46**, 1059 (2004).
S6. R. E. M. Rickaby, H. Elderfield, *Geochem. Geophys. Geosys.* **6**, doi:10.1029/2004GC000858 (2005).
S7. J. F. McManus, R. Francois, J. M. Gherardi, L. D. Keigwin, S. Brown-Leger, *Nature* **428**, 834 (2004).
S8. N. J. Shackleton, M. A. Hall, E. Vincent, *Paleoceanography* **15**, 565 (2000).
S9. T. Blunier, E. J. Brook, *Science* **291**, 109 (2001).
S10. S. H. H. Nielsen, D. A. Hodell, G. Kamenov, T. Guilderson, M. R. Perfit, *Geochemistry Geophysics Geosystems* **8**, Q12005 (2007).